Manganese(II) and Iron(III) Complexes of the Tridentate Ligands Bis(benzimidazol-2-ylmethyl)-amine (L^1) and -methylamine (L^2). Crystal Structures of $[MnL^1(CH_3CO_2)_2]$, $[FeL^2Cl_3]$, and $[Fe_2L^1_2(\mu\text{-}O)\{\mu\text{-}(CH_3)_3CCO_2\}_2][ClO_4]_2$†

Harry Adams, Neil A. Bailey,* Jonathan D. Crane, and David E. Fenton*
Department of Chemistry, The University, Sheffield S3 7HF
Jean-Marc Latour
Laboratoire de Chemie (UA 1194), Departement de Recherche Fondamentale, Centre d'Etudes Nucleaires de Grenoble, 85X, 30841 Grenoble Cedex, France
John M. Williams
Department of Physics, The University, Sheffield S3 7HF

The preparation and characterisation of $[MnL^1(CH_3CO_2)_2]$ (**1**), $[Mn_6(\mu_4\text{-}O)_2(C_6H_5CO_2)_{10}(H_2O)_4]$ (**9**), $[FeL^1Cl_3]$ (**10**), $[FeL^2Cl_3]$ (**2**), and $[Fe_2L^1_2(\mu\text{-}O)\{\mu\text{-}(CH_3)_3CCO_2\}_2][ClO_4]_2$ (**3**) are reported where L^1 and L^2 are bis(benzimidazol-2-ylmethyl)amine and bis(benzimidazol-2-ylmethyl)methylamine. The molecular structures of (**1**), (**2**), and (**3**) were determined by *X*-ray diffraction. Complex (**1**) exists as a discrete, neutral, mononuclear species in the solid state. The manganese(II) ion is five-co-ordinate with the tridentate ligand bound in a meridional manner. Both acetates are monodentate with Mn–O distances of 2.076(5) and 2.158(5) Å. Complex (**9**) contains a $[Mn_6(\mu_4\text{-}O)_2]^{10+}$ core, formally $4Mn^{II}:2Mn^{III}$. Complex (**2**) is neutral, mononuclear, distorted octahedral. The ligand co-ordinates in a similar manner to that seen in (**1**) and the chlorides occupy the three remaining meridional sites, with Fe–Cl(equatorial) 2.318(5) Å and Fe–Cl(axial) 2.322(5) and 2.433(5) Å. The Mössbauer spectrum of (**10**) at room temperature comprises a quadrupole doublet: $\delta = 0.40(1)$, $\Delta E_Q = 0.33(2)$ mm s^{-1}. Complex (**3**) is a dinuclear iron(III) species containing the triply bridged $[Fe_2(\mu\text{-}O)(\mu\text{-}RCO_2)_2]^{2+}$ core. The Fe · · · Fe distance is 3.075(5) Å and the Fe–O(oxo)–Fe angle is 117.0(6)°. The high-spin iron(III) centres are antiferromagnetically coupled with $J = -116$ cm^{-1}. The Mössbauer spectra of (**3**) at room temperature and 70 K consist of doublets with $\delta = 0.44(1)$, $\Delta E_Q = 1.37(2)$, and $\delta = 0.55(1)$, $\Delta E_Q = 1.30(2)$ mm s^{-1} respectively.

Multinuclear iron and manganese cores are believed to be present in the active sites of several metalloproteins. Dinuclear iron systems include haemerythrin (Figure 1), methane monooxygenase, and ribonucleotide reductase.[1] The pseudocatalase from *Lactobacillus plantarum* is postulated to contain a dinuclear manganese(III) core,[2] and the dioxygen-evolving complex of photosystem II may contain up to four manganese ions.[3] The co-ordination environments of the metal ions in these biosites are dominated by imidazole (histidine) and carboxylate (aspartate and glutamate) residues. To understand the chemistry of the assembly and function of these metalloproteins it is logical to prepare potential model compounds by utilising ligands containing the imidazole moiety. Thus the co-ordination of iron(III) and manganese(II) ions with bis(benzimidazol-2-ylmethyl)amine (L^1) and bis(benzimidazol-2-ylmethyl)methylamine (L^2) in the presence of simple carboxylic acids was investigated.

These ligands are capable of co-ordinating a transition metal in two distinct ways, either meridionally or facially. In the complexes described here meridional co-ordination is observed in the mononuclear complexes $[MnL^1(CH_3CO_2)_2]$ (**1**) and $[FeL^2Cl_3]$ (**2**), and facial co-ordination in the dinuclear complex $[Fe_2L^1_2(\mu\text{-}O)\{\mu\text{-}(CH_3)_3CCO_2\}_2][ClO_4]_2$ (**3**).

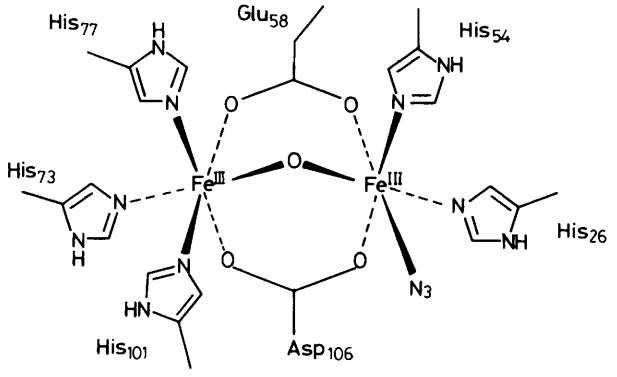

Figure 1. Schematic of the dinuclear iron(III) core of azidomethaemerythrin

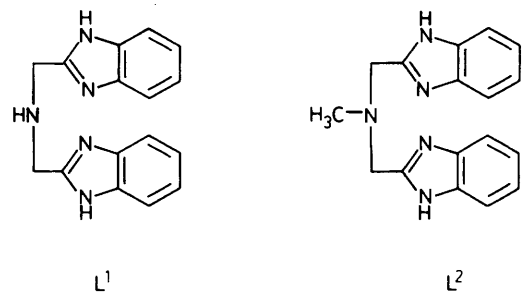

L^1 L^2

Many manganese(II) complexes of the general formula $[MnLX_2]$ with L being a tridentate N_3 ligand are known,

† Diacetato[bis(benzimidazol-2-ylmethyl)amine-$NN^3N^{3'}$]-manganese(II), [bis(benzimidazol-2-ylmethyl)methylamine-$NN^3N^{3'}$]-trichloroiron(III), and μ-oxo-di-μ-pivalato-bis{[bis(benzimidazol-2-ylmethyl)amine-$NN^3N^{3'}$]iron(III)}.

Supplementary data available: see Instructions for Authors, *J. Chem. Soc., Dalton Trans.*, 1990, Issue 1, pp. xix—xxii.

although none has been reported for which X is a carboxylate anion. To date the structures of these compounds have been elucidated by comparison of *X*-ray powder diffraction patterns with those of isomorphous complexes of other transition metals of known structure.[4] The molecular structure of the five-co-ordinate complex (**1**) was determined by single-crystal *X*-ray diffraction.

Octahedral iron(III) complexes with N_3Cl_3 donor sets display either facial or meridional co-ordination of the chlorides depending upon the nature of the other ligand(s).[5,6] Due to the planar geometry of L^2 in (**2**) the chlorides are bound meridionally.

Crystallographic studies of met- and azidomet-haemerythrin confirm the presence of the $[Fe_2(\mu\text{-}O)(\mu\text{-}RCO_2)_2]^{2+}$ core (Figure 1).[7] Several tridentate, facially co-ordinating ligands have been used to prepare model compounds incorporating this core: 1,4,7-triazacyclononane (L^3),[8] 1,4,7-trimethyl-1,4,7-triazacyclononane (L^4),[9] the hydrotris(pyrazolyl)borate anion (L^5),[10] *N,N,N',N'*-tetra(2'-pyridylmethyl)-1,4-diaminobutane (L^6) and its 1,3-diaminopropane analogue (L^7),[11] as well as the bidentate ligand 2,2'-bipyridyl (L^8).[12] The dinuclear iron(III) complexes $[Fe_2L^3{}_2O(CH_3CO_2)_2]I_2$ (**4**), $[Fe_2L^4{}_2O(CH_3CO_2)_2][ClO_4]_2$ (**5**), $[Fe_2L^5{}_2O(CH_3CO_2)_2]$ (**6**), $[Fe_4L^6{}_2O_2(CH_3CO_2)_4][NO_3]_4$ (**7**), and $[Fe_2L^8{}_2Cl_2O(CH_3CO_2)_2]$ (**8**) of these ligands are all model compounds for azidomethaemerythrin but until recently none contained the biologically relevant imidazole moiety. Complexation of L^1, however, gave the analogous dinuclear iron(III) species (**3**).

Experimental

Preparation.—1,2-Diaminobenzene was recrystallised before use.[13] *N*-Methyliminodiacetic acid was prepared by the literature method.[14] All other reagents and solvents were used without further purification.

CAUTION: Although no problems were encountered in the preparation of the perchlorate salt (**3**), suitable care should be taken when handling such potentially hazardous compounds.

Bis(benzimidazol-2-ylmethyl)amine monohydrate $L^1{\cdot}H_2O$. Iminodiacetic acid (13.3 g, 0.1 mol) and 1,2-diaminobenzene (20.2 g, 0.2 mol) were intimately mixed and heated to 180—200 °C (oil-bath) in an open flask. When no further steam was evolved the melt was allowed to cool. The dark glassy solid was taken up in hot hydrochloric acid (4 mol dm^{-3}, 200 cm^3) and filtered. After cooling, the trihydrochloride salt of L^1 precipitated as a pale blue, feathery solid. This was taken up in warm water (200 cm^3), KOH (28.0 g, 0.5 mol) added, and the solution brought to reflux. Methanol was added until the precipitate redissolved. After refluxing with decolorising charcoal (15 min) the solution was filtered and gave the crude, free amine upon cooling. Two recrystallisations from methanol–water gave $L^1{\cdot}H_2O$ as white needles (10.6 g, 36%), m.p. 270 °C (decomp.) (Found: C, 65.20; H, 5.80; N, 23.70. $C_{16}H_{17}N_5O$ requires C, 65.10; H, 5.80; N, 23.70%); *m/z* (chemical ionisation, c.i.) 278 (MH^+, 55%); δ(H)(CD_3OD) 7.52 (4 H, m, aryl H), 7.19 (4 H, m, aryl H), and 4.09 (4 H, s, CH_2).

Bis(benzimidazol-2-ylmethyl)methylamine (L^2). This was prepared by the same method as for L^1 but using *N*-methyliminodiacetic acid. Pale pink needles (4.20 g, 15%), m.p. 280 °C (decomp.) (Found: C, 70.10; H, 6.10; N, 24.10. $C_{17}H_{17}N_5$ requires C, 70.10; H, 5.90; N, 24.00%); *m/z* (c.i.) 292 (MH^+, 100%). δ_H(CD_3OD) 7.58 (4 H, m, aryl H), 7.23 (4 H, m, aryl H), 3.96 (4 H, s, CH_2), and 2.31 (3 H, s, CH_3).

$[MnL^1(CH_3CO_2)_2]$ (**1**). The ligand $L^1{\cdot}H_2O$ (0.29 g, 1 mmol) and manganese(II) acetate tetrahydrate (0.25 g, 1 mmol) were suspended in refluxing acetonitrile (30 cm^3). Methanol was added dropwise until all the solid dissolved. The solution was filtered hot and allowed to cool. Pale yellow-brown crystals formed over a few days. The product was filtered off, washed with ethanol then diethyl ether, and air dried (0.23 g, 51%) (Found: C, 53.10; H, 4.80; N, 15.60. $C_{20}H_{21}MnN_5O_4$ requires C, 53.30; H, 4.70; N, 15.55%).

$[Mn_6(\mu_4\text{-}O)_2(C_6H_5CO_2)_{10}]{\cdot}4H_2O$ (**9**). The ligand $L^1{\cdot}H_2O$ (0.29 g, 1 mmol), sodium benzoate (0.14 g, 1 mmol), and manganese(II) perchlorate (0.37 g, 1 mmol) were dissolved in refluxing acetonitrile (25 cm^3). The solution was cooled to room temperature and filtered. Over a period of 48 h the pale solution darkened and golden-yellow rod-like crystals of complex (**2**) were deposited. These were filtered off, washed with acetonitrile, and air dried (0.085 g, 31%) (Found: C, 51.10; H, 3.45; N, negative. $C_{70}H_{58}Mn_6O_{26}$ requires C, 51.10; H, 3.55%).

$[FeL^1Cl_3]$ (**10**). The ligand $L^1{\cdot}H_2O$ (0.29 g, 1 mmol) and iron(III) chloride hexahydrate (0.27 g, 1 mmol) were dissolved in ethanol (40 cm^3). The deep red, clear solution was filtered and red microcrystals were deposited after a few hours. The product was filtered off, washed with ethanol then diethyl ether, and dried *in vacuo* (0.33 g, 75%) (Found: C, 43.85; H, 3.60; Cl, 23.75; N, 15.90. $C_{16}H_{15}Cl_3FeN_5$ requires C, 43.70; H, 3.40; Cl, 24.20; N, 15.90%).

$[FeL^2Cl_3]{\cdot}CH_3OH$ (**2**)·CH_3OH. The ligand L^2 (0.29 g, 1 mmol) and iron(III) chloride hexahydrate (0.27 g, 1 mmol) were dissolved in methanol (40 cm^3). The deep red, clear solution was filtered and crystals of complex (**4**)·CH_3OH were deposited over a few weeks (0.19 g, 39%) (Found: C, 44.60; H, 4.50; Cl, 21.70; N, 14.40. $C_{18}H_{21}Cl_3FeN_5O$ requires C, 44.50; H, 4.40; Cl, 21.90; N, 14.40%).

$[Fe_2L^1{}_2(\mu\text{-}O)\{\mu\text{-}(CH_3)_3CCO_2\}_2][ClO_4]_2$ (**3**). This was prepared by two different methods.

Method (*a*). The ligand $L^1{\cdot}H_2O$ (0.28 g, 1 mmol) and iron(III) perchlorate decahydrate (0.54 g, 1 mmol) were dissolved in ethanol (40 cm^3) to give a deep red solution. Pivalic acid (0.30 g, 3 mmol) then tri-n-butylamine (0.57 g, 3 mmol) were added with stirring and the solution became deep green in colour (*ca.* 5 min). Diethyl ether (40 cm^3) was added slowly with stirring. The resulting solution was filtered and allowed to stand. Large dark green crystals of complex (**3**) formed overnight. The product was filtered off, washed with ethanol then diethyl ether, and air dried (0.18 g, 33%) (Found: C, 46.50; H, 4.50; Cl, 6.50, N, 12.70. $C_{42}H_{48}Cl_2Fe_2N_{10}O_{13}$ requires C, 46.60; H, 4.50; Cl, 6.50; N, 12.90%).

Method (*b*). Pivalic acid (0.30 g, 3 mmol) and tri-n-butylamine (0.57 g, 3 mmol) were added to a suspension of complex (**10**) (0.44 g, 1 mmol) in ethanol (40 cm^3). The mixture was brought to reflux and water added dropwise until a deep green, clear solution was formed. Saturated ethanolic sodium perchlorate (*ca.* 2 cm^3) was added and complex (**3**) was isolated from the resulting solution as for method (*a*).

Magnetic Studies.—Magnetic susceptibility measurements were carried out using a variable-temperature superconducting magnetometer SHE 900 operating at 5 kG (0.5 T) in the range 5—300 K. The sample (**3**) was constituted of a few crystals (weight 18.2 mg) contained in a KelF bucket which was calibrated independently. The diamagnetic correction was evaluated, 555×10^{-6} cm^3 mol^{-1}, using Pascal's constants. The data were fitted by the equation for two interacting iron(III) ions derived from the usual Hamiltonian $H_0 = -2JS_1S_2$.[15] This equation was modified to include the contributions of a high-spin iron(III) contaminant exhibiting Curie behaviour and the temperature-independent paramagnetism (t.i.p.) [equation (1)] where $\mathcal{N}$, k, and β have their usual meaning, and ν was the mole fraction of iron(III) contaminant. The value minimised was $R = \Sigma(\chi_{expl.} - \chi_{calc.})^2/N\Sigma(\chi_{expl.})^2$, where N is the number of data (63). Each data point was the mean of 10 measurements. The best R index, 8.5×10^{-7}, was obtained for the following

Table 1. Summary of crystal data for complexes (**1**), (**2**), and (**3**)

Compound	(**1**)	(**4**)	(**5**)
Formula	$C_{20}H_{21}MnN_5O_4$	$C_{18}H_{21}Cl_3FeN_5O$	$C_{42}H_{48}Cl_2Fe_2N_{10}O_{13}$
Crystal size/mm	0.39 × 0.24 × 0.02	0.35 × 0.25 × 0.23	0.48 × 0.20 × 0.20
M	450.35	485.60	1 083.50
Symmetry	Triclinic	Monoclinic	Tetragonal
Space group	$P\bar{1}(C_i$, no. 2)	$P2_1/c(C_{2h}^5$, no. 14)	$P4_2/n(C_{4h}^4$, no. 86)
a/Å	9.240(12)	10.035(22)	14.77(3)
b/Å	10.018(21)	15.297(33)	
c/Å	12.778(30)	14.197(18)	24.67(4)
α/°	65.83(16)		
β/°	83.67(17)	99.75(14)	
γ/°	70.23(14)		
U/Å^3	1 015(4)	2 148(7)	5 381(17)
Z	2	4	4
F(000)	465.89	995.79	2 239.54
D_c/g cm^{-3}	1.474	1.502	1.337
μ/cm^{-1}	6.59	10.96	7.01
Final *R*	0.0505	0.0653	0.0829
No. reflections used	2 728	2 607	1 893

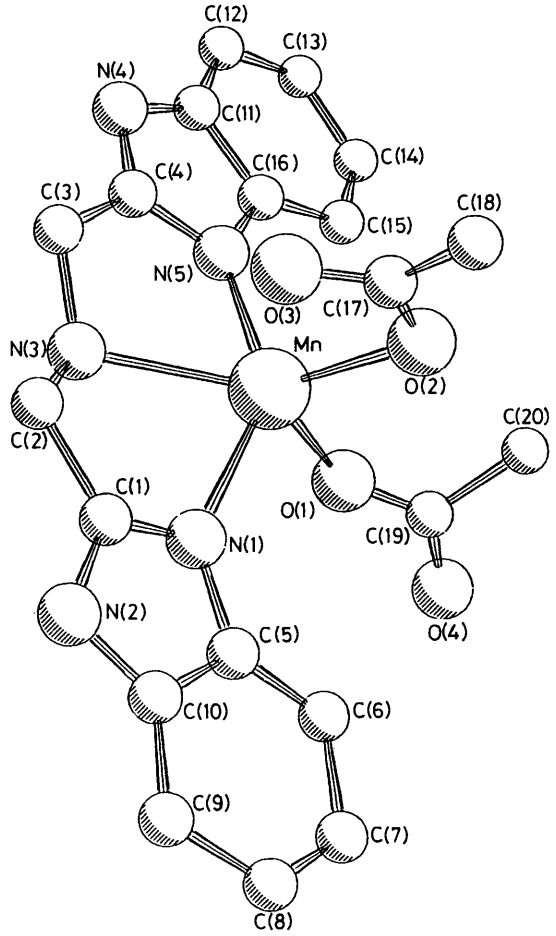

Figure 2. Molecular geometry of complex (**1**). Selected bond lengths and angles are given in Table 2

parameters: $g = 2.04$, $p = 7 \times 10^{-4}$, t.i.p. = 24×10^{-6} cm^3 mol^{-1}, and $J = -116$ cm^{-1}.

$$\chi_{calc.} = p\frac{35\mathcal{N}\beta^2}{3kT} + (1-p)\frac{\mathcal{N}g^2\beta^2}{kT} \cdot \frac{2e^{2x} + 10e^{6x} + 28e^{12x} + 60e^{20x} + 110e^{30x}}{1 + 3e^{2x} + 5e^{6x} + 7e^{12x} + 9e^{20x} + 11e^{30x}} + \text{t.i.p.} \quad (1)$$

Mössbauer Studies.—Transmission Mössbauer spectra were recorded using a conventional constant-acceleration spectrometer and a multi-channel analyser. The absorber was mounted in a continuous-flow helium cryostat capable of stabilising the temperature anywhere between room temperature and 4.2 K. Generally spectra were taken at room temperature and at 70 K. A 25-mC ^{57}Co(Rh) source was used throughout but all isomer shift values (δ) quoted are relative to standard α-iron at room temperature. The data were subsequently fitted using a least-squares minimising program which allowed any desired combination of Lorentzian line shapes to be superimposed. Spectra are shown as measured, together with the resulting line fit.

X-Ray Crystallography.—Three-dimensional, room-temperature *X*-ray data were collected in the range $3.5 < 2\theta < 50°$ on a Nicolet R3 diffractometer by the ω-scan method (Table 1), using Mo-K_α radiation ($\bar{\lambda} = 0.710\,69$ Å). The independent reflections ($|F|/\sigma(|F|) > 3.0$ for complexes (**1**) and (**2**) $|F|/\sigma(|F|) > 4.0$ for (**3**)] were corrected for Lorentz and polarisation effects, and for absorption by analysis of azimuthal scans. The structures were solved by Patterson and Fourier techniques and refined by blocked-cascade least-squares methods. Hydrogen atoms were included in calculated positions with isotropic thermal parameters related to those of the supporting atom. Refinement converged to the final *R* values given, with allowance for the thermal anisotropy of all non-hydrogen atoms. Complex scattering factors were taken from the program package SHELTXL[16] as implemented on a Data General Nova 3 computer. For complex (**1**) the weighting scheme was $w = [\sigma^2(F) + gF^2]^{-1}$, where $g = 0.000\,49$. For (**2**) and (**3**) unit weights were used throughout. The crystal data are summarised in Table 1.

Additional material available from the Cambridge Crystallographic Data Centre comprises H-atom co-ordinates, thermal parameters, and remaining bond lengths and angles.

Results and Discussion

$[MnL^1(CH_3CO_2)_2]$ (**1**) *and* $[Mn_6(\mu_4\text{-}O)_2(C_6H_5CO_2)_{10}(H_2O)_4]$ (**9**).—In complex (**1**) the manganese(II) ion is five-co-ordinate with L^1 adopting a near-planar geometry and thus co-ordinating meridionally. The molecular geometry is shown in Figure 2 and structural data given in Tables 2 and 3. It is likely that the ligand maintains a planar geometry upon dissolution and does not adopt the alternative facial mode of co-

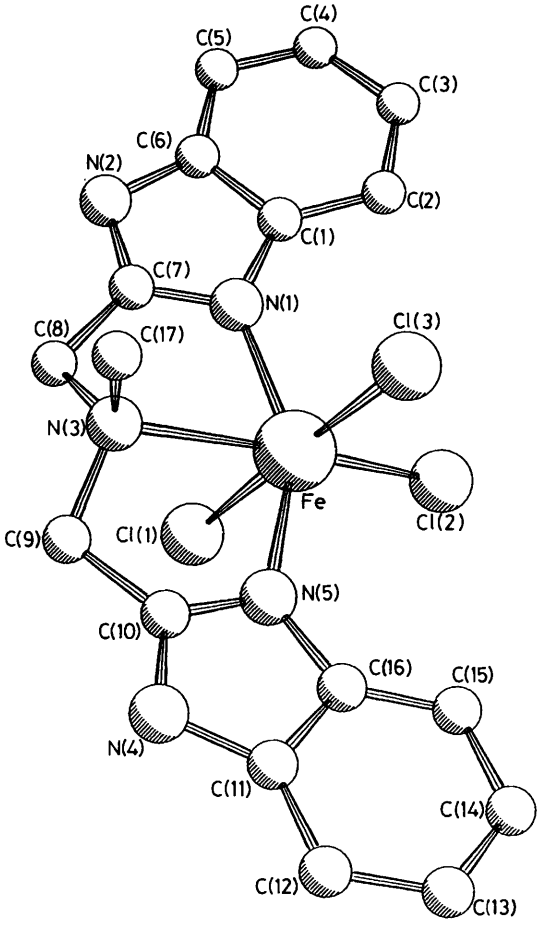

Figure 3. Molecular geometry of complex (**2**). Selected bond lengths and angles are given in Table 5

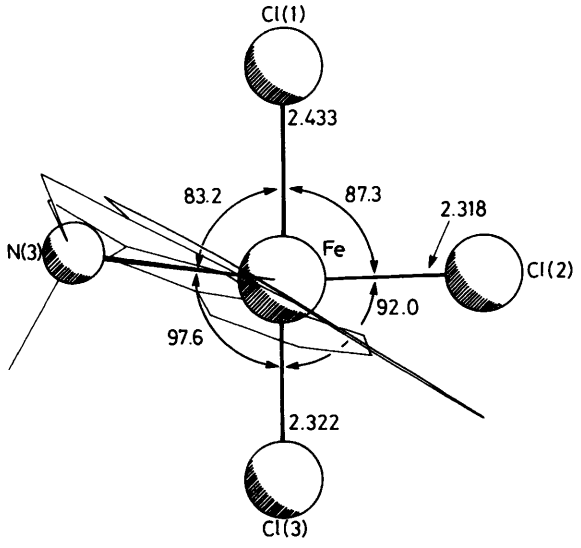

Figure 4. View of the ligand-imposed distortion of the planar $NFeCl_3$ fragment of (**2**); distances in Å, angles in °

ordination since methanolic solutions of (**1**) are stable in air over periods of several weeks. In contrast solutions of manganese(II) ions with facially co-ordinating N_2 donor ligands in the presence of carboxylate groups contain the air-sensitive $[Mn_2L_2(\mu\text{-}OH)(\mu\text{-}RCO_2)_2]^+$ moiety.[17]

However, with only 1 equivalent of benzoate per manganese(II) in methanolic solution, partial oxidation occurs to give complex (**9**) in which two of the manganese ions are formally in the +3 oxidation state. Similar clusters with carboxylate bridges have previously been reported.[18,19] The $[Mn_6(\mu_4\text{-}O)_2]^{10+}$ core consists of two $Mn_4(\mu_4\text{-}O)$ tetrahedra sharing an edge. Crystals of suitable quality for an *X*-ray diffraction structure determination could not be prepared. However, the positive-ion fast-atom bombardment (f.a.b.) mass spectrum confirms the hexanuclear nature of the complex. The four water molecules are readily lost and not observed, thus the highest-mass peak of significance corresponds to $[Mn_6O_2(C_6H_5CO_2)_{10}]^+$ (*m/z* 1 572). The i.r. spectrum is dominated by benzoate peaks with the antisymmetric and symmetric modes of the bridging carboxylates occurring at $\nu_{max.}$ = 1 580 and 1 400 cm^{-1} respectively. Interestingly the ligand is not present in the product and probably only behaves as a weak base in the reaction mixture. Repetition of the reaction with 3 equivalents of triethylamine instead of L^1 still gave microcrystals of (**9**), but in reduced yield.

In the molecular structure of complex (**1**) each benzimidazole group is virtually planar and the angle between the planes is 3.3°. A direct result of the coplanar nature of L^1 is that the central secondary amine donor is significantly further from the manganese(II) ion than the benzimidazole nitrogens: Mn–N(benzimidazole) 2.195, 2.223; Mn–N(amine) 2.358 Å. One acetate group is purely monodentate with a Mn–O distance of 2.076 Å. The other is primarily monodentate, Mn–O 2.158 Å, but the 'keto' oxygen is directed back towards the metal with a long Mn–O interaction of 2.618 Å. In addition both acetates are hydrogen bonded to N–H groups of neighbouring molecules. In the i.r. spectrum (KBr disc) the antisymmetric and symmetric stretching modes of the acetates occur at 1 565 and 1 440 cm^{-1}.

Although this complex exists as discrete monomers in the solid state, medium-intensity peaks of high mass are observed in the positive-ion f.a.b. mass spectrum. Assignments of these as aggregates of ligand, manganese ions, and acetate groups are given in Table 4. Presumably these aggregates are formed upon dissolution of the complex in the matrix solvent. Attempts to produce a manganese(III) analogue of (**3**) by reaction of L^1 with manganese(III) acetate[20] failed; insoluble, brown powders were isolated, the i.r. spectra of which showed that L^1 was not present.

$[FeL^1Cl_3]$ (**10**) *and* $[FeL^2Cl_3]\cdot CH_3OH$, (**2**)$\cdot CH_3OH$.—Conductivity measurements for (**10**) in methanol show that this complex exists as a 1:1 electrolyte in solution but neither details of its preparation nor its structure in the solid state have been reported.[21] Crystals of (**10**) of sufficient quality for an *X*-ray diffraction structure determination could not be obtained. Use of the *N*-methyl derivative of the ligand, however, enabled the preparation of red crystals of (**2**)$\cdot CH_3OH$. It is reasonable to assume that both (**10**) and (**2**) have similar molecular structures. In complex (**2**) the ligand co-ordinates in a meridional fashion as in (**1**). The molecular geometry of (**2**) is shown in Figure 3 and structural data given in Tables 5 and 6. The two benzimidazole groups are not as coplanar as observed for (**1**), the angle between the least-squares planes being 17°. The iron(III) ion is six-co-ordinate with a distorted octahedral geometry. The chloride ligands occupy the three remaining meridional sites. As in (**1**) the central nitrogen of the ligand is furthest from the metal: Fe–N(benzimidazole) 2.082, 2.104; Fe–N(amine) 2.374 Å. The shortest Fe–Cl distance is to the chloride in the plane of the ligand: Fe–Cl(equatorial) 2.318; Fe–Cl(axial) 2.322, 2.433 Å. The orientation of the ligand sterically dictates that the Cl(1)–Fe–N(3) and Cl(1)–Fe–Cl(2) bond angles are significantly less than 90° (Figure 4). This angular compression is directly linked with the large asymmetry in the Fe–Cl(axial) distances.

Several iron(III) complexes with N_3Cl_3 co-ordination are known and both meridional and facial co-ordination of the

Table 2. Selected bond lengths (Å) and angles (°) for complex (**1**) with standard deviations in parentheses

Mn–N(1)	2.223(5)	Mn–N(3)	2.358(5)	C(5)–C(6)	1.395(7)	C(15)–C(16)	1.385(6)
Mn–N(5)	2.195(5)	Mn–O(1)	2.076(5)	C(5)–C(10)	1.396(6)	C(11)–C(16)	1.409(6)
Mn–O(2)	2.158(5)	Mn ... O(3)	2.618(5)	C(6)–C(7)	1.379(7)	C(14)–C(15)	1.376(6)
N(1)–C(1)	1.325(5)	N(5)–C(4)	1.332(6)	C(7)–C(8)	1.391(7)	C(13)–C(14)	1.404(8)
N(1)–C(5)	1.405(6)	N(5)–C(16)	1.396(5)	C(8)–C(9)	1.381(8)	C(12)–C(13)	1.366(7)
N(2)–C(1)	1.346(5)	N(4)–C(4)	1.339(6)	C(9)–C(10)	1.393(7)	C(11)–C(12)	1.389(6)
N(2)–C(10)	1.386(6)	N(4)–C(11)	1.385(5)	O(2)–C(17)	1.252(6)	O(1)–C(19)	1.262(5)
N(3)–C(2)	1.461(5)	N(3)–C(3)	1.467(6)	O(3)–C(17)	1.246(5)	O(4)–C(19)	1.233(7)
C(1)–C(2)	1.496(7)	C(3)–C(4)	1.497(6)	C(17)–C(18)	1.497(6)	C(19)–C(20)	1.495(7)
O(1)–Mn–O(2)	98.1(2)	N(1)–Mn–N(5)	141.6(1)	N(2)–C(10)–C(5)	105.4(4)	N(4)–C(11)–C(16)	105.3(3)
O(1)–Mn–N(1)	91.8(2)	O(1)–Mn–N(5)	101.2(2)	N(2)–C(10)–C(9)	132.1(4)	N(4)–C(11)–C(12)	133.0(4)
O(2)–Mn–N(1)	106.7(2)	O(2)–Mn–N(5)	107.0(2)	C(1)–N(1)–C(5)	105.0(3)	C(4)–N(5)–C(16)	104.7(3)
O(1)–Mn–N(3)	130.9(1)	O(2)–Mn–N(3)	130.8(2)	C(1)–N(2)–C(10)	107.6(3)	C(4)–N(4)–C(11)	107.5(3)
N(1)–Mn–N(3)	72.2(2)	N(3)–Mn–N(5)	72.0(1)	C(2)–N(3)–C(3)	115.2(4)		
Mn–N(1)–C(1)	113.4(3)	Mn–N(5)–C(4)	115.4(3)	O(1)–C(19)–O(4)	123.1(4)	O(2)–C(17)–O(3)	120.2(3)
Mn–N(1)–C(5)	138.8(2)	Mn–N(5)–C(16)	139.1(3)	O(1)–C(19)–C(20)	117.8(5)	O(2)–C(17)–C(18)	120.2(3)
Mn–N(3)–C(2)	108.2(2)	Mn–N(3)–C(3)	109.1(2)	O(4)–C(19)–C(20)	119.1(4)	O(3)–C(17)–C(18)	119.6(4)
Mn–O(1)–C(19)	139.5(3)	Mn–O(2)–C(17)	104.3(2)	C(6)–C(5)–C(10)	119.7(4)	C(11)–C(16)–C(15)	120.6(4)
N(1)–C(1)–N(2)	112.8(4)	N(4)–C(4)–N(5)	113.3(3)	C(5)–C(6)–C(7)	117.8(4)	C(14)–C(15)–C(16)	117.5(4)
N(1)–C(1)–C(2)	122.6(3)	N(5)–C(4)–C(3)	121.8(4)	C(6)–C(7)–C(8)	122.1(5)	C(13)–C(14)–C(15)	121.4(4)
N(2)–C(1)–C(2)	124.5(3)	N(4)–C(4)–C(3)	124.8(4)	C(7)–C(8)–C(9)	121.1(5)	C(12)–C(13)–C(14)	121.9(4)
N(3)–C(2)–C(1)	107.8(3)	N(3)–C(3)–C(4)	107.1(4)	C(8)–C(9)–C(10)	116.9(4)	C(11)–C(12)–C(13)	116.8(4)
N(1)–C(5)–C(6)	131.2(4)	N(5)–C(16)–C(15)	130.3(4)	C(5)–C(10)–C(9)	122.5(4)	C(12)–C(11)–C(16)	121.7(4)
N(1)–C(5)–C(10)	109.1(4)	N(5)–C(16)–C(11)	109.1(3)				

Table 3. Final fractional atomic co-ordinates ($\times 10^4$) for complex (**1**), with estimated standard deviations in parentheses

Atom	*x*	*y*	*z*
Mn	3 401(1)	1 378(1)	3 264(1)
O(1)	4 783(3)	2 679(3)	3 174(2)
O(2)	1 671(3)	3 157(3)	1 989(3)
O(3)	836(3)	1 197(3)	2 734(2)
O(4)	5 467(4)	4 631(3)	3 052(3)
N(1)	2 531(3)	1 386(3)	4 955(2)
N(2)	1 127(3)	461(3)	6 434(2)
N(3)	3 549(3)	−1 176(3)	4 497(2)
N(4)	5 379(3)	−2 336(3)	2 187(2)
N(5)	4 861(3)	−169(3)	2 470(2)
C(1)	1 975(4)	243(4)	5 556(3)
C(2)	2 244(4)	−1 114(4)	5 254(3)
C(3)	3 657(4)	−2 067(4)	3 805(3)
C(4)	4 634(4)	−1 527(4)	2 809(3)
C(5)	1 992(4)	2 432(4)	5 491(3)
C(6)	2 227(4)	3 831(4)	5 253(3)
C(7)	1 521(5)	4 620(5)	5 937(4)
C(8)	604(5)	4 060(5)	6 838(4)
C(9)	374(5)	2 667(5)	7 096(3)
C(10)	1 088(4)	1 870(4)	6 407(3)
C(11)	6 185(4)	−1 471(4)	1 370(3)
C(12)	7 150(4)	−1 727(4)	509(3)
C(13)	7 819(5)	−627(5)	−114(3)
C(14)	7 554(5)	702(5)	102(3)
C(15)	6 559(4)	985(4)	927(3)
C(16)	5 861(4)	−113(4)	1 563(3)
C(17)	646(4)	2 566(4)	2 065(3)
C(18)	−820(5)	3 504(5)	1 361(4)
C(19)	4 823(4)	4 041(4)	2 650(3)
C(20)	4 084(7)	4 955(5)	1 475(4)

three chloride ligands has been observed. Both geometries are observed in the related 1,10-phenanthroline (phen) complexes *fac*-[$FeCl_3$(phen)(CH_3OH)] and *mer*-[$FeCl_3$(phen){$(CH_3)_2$NCHO}].[22,23] The arrangement of the chloride ligands in these systems is apparently solely dependent upon the stereochemical requirements of the other ligands. Thus the structure of this complex confirms that ligands of this type preferentially adopt a near-planar geometry upon co-ordination.

Table 4. Assignments of the high-mass aggregate peaks in the positive-ion f.a.b. mass spectrum of [$MnL^1(CH_3CO_2)_2$] (**1**)

[fragment]$^+$	*m/z* (% intensity)*
[$Mn_2L^1_2(CH_3CO_2)_2 - H$]	781 (9)
[$Mn_2L^1_2(CH_3CO_2) - 2H$]	721 (15)
[$MnL^1_2 - H$]	608 (18)
[$MnL^1(CH_3CO_2)$]	391 (100)
[$MnL^1 - H$]	331 (68)

* 3-Nitrobenzyl alcohol matrix.

The positive-ion f.a.b. mass spectra (3-nitrobenzyl alcohol matrix) of complexes (**10**) and (**2**) are straightforward with parent peaks of *m/z* 403, [FeL^1Cl_2]$^+$, and 417, [FeL^2Cl_2]$^+$, respectively. Unlike (**1**) there are no high-mass aggregate peaks of any significance. The electronic spectra of (**10**) and (**2**) in methanol show charge-transfer bands at $\lambda_{max.}$ = 356 (ε = 2 935) and 365 nm (3 383 $dm^3\ mol^{-1}\ cm^{-1}$ per Fe) respectively.

The room-temperature Mössbauer spectrum of complex (**10**) consists of an asymmetric quadrupole doublet (fitted as two singlets of identical linewidth but variable intensity) with isomer shift, δ = 0.40(1) mm s^{-1} and quadrupole splitting, ΔE_Q = 0.33(2) mm s^{-1} (Figure 5). These values are comparable with those of other $FeCl_3$ adducts and are consistent with high-spin iron(III) in a single metal environment.[6]

[$Fe_2L^1_2(\mu$-O){μ-$(CH_3)_3CCO_2$}$_2$][ClO_4]$_2$ (**3**).—The dication in complex (**3**) contains the [$Fe_2(\mu$-O)(μ-$RCO_2)_2$]$^{2+}$ core known to occur in the met and azidomet forms of haemerythrin.[7] The molecular structure of (**3**) is shown in Figure 6 and structural data given in Tables 7 and 8. The stability of this dinuclear iron(III) moiety is underlined by the spontaneous self assembly of (**3**) either directly [method (*a*)] or from the $FeCl_3$ complex (**10**) [method (*b*)]. To allow the accommodation of this core the ligand has adopted the facially co-ordinating geometry not observed in the mononuclear complexes (**1**) and (**2**). Thus the preparation of (**3**) from (**10**) must involve the ligand switching from meridional to facial co-ordination during the assembly of the triply bridged core. This dinuclear iron(III) species is a homologue of the previously reported [$Fe_2L^1_2(\mu$-O)-

Table 5. Selected bond lengths (Å) and angles (°) for complex (**2**) with standard deviations in parentheses

Fe–Cl(1)	2.433(5)	Fe–Cl(2)	2.318(5)	N(5)–C(10)	1.306(9)	N(5)–C(16)	1.411(9)
Fe–Cl(3)	2.322(5)	Fe–N(1)	2.082(8)	C(1)–C(2)	1.392(12)	C(1)–C(6)	1.407(11)
Fe–N(3)	2.374(7)	Fe–N(5)	2.104(7)	C(2)–C(3)	1.413(14)	C(3)–C(4)	1.401(15)
N(1)–C(1)	1.413(11)			C(4)–C(5)	1.361(15)	C(5)–C(6)	1.415(13)
N(1)–C(7)	1.322(10)	N(2)–C(6)	1.398(11)	C(7)–C(8)	1.497(12)	C(9)–C(10)	1.486(10)
N(2)–C(7)	1.357(11)	N(3)–C(8)	1.476(10)	C(11)–C(12)	1.401(12)	C(11)–C(16)	1.412(11)
N(3)–C(9)	1.494(10)	N(3)–C(17)	1.484(10)	C(12)–C(13)	1.375(11)	C(13)–C(14)	1.422(13)
N(4)–C(10)	1.361(10)	N(4)–C(11)	1.383(9)	C(14)–C(15)	1.382(12)	C(15)–C(16)	1.387(10)
Cl(1)–Fe–Cl(2)	87.3(1)	Cl(1)–Fe–Cl(3)	178.6(1)	N(1)–C(1)–C(6)	108.5(7)	C(2)–C(1)–C(6)	120.8(8)
Cl(2)–Fe–Cl(3)	92.0(1)	Cl(1)–Fe–N(1)	88.9(2)	C(1)–C(2)–C(3)	117.0(8)	C(2)–C(3)–C(4)	120.9(9)
Cl(2)–Fe–N(1)	103.8(2)	Cl(3)–Fe–N(1)	92.4(2)	C(3)–C(4)–C(5)	122.9(10)	C(4)–C(5)–C(6)	116.6(9)
Cl(1)–Fe–N(3)	83.2(2)	Cl(2)–Fe–N(3)	170.1(2)	N(2)–C(6)–C(1)	105.7(7)	N(2)–C(6)–C(5)	132.4(8)
Cl(3)–Fe–N(3)	97.6(2)	N(1)–Fe–N(3)	73.3(3)	C(1)–C(6)–C(5)	121.8(8)	N(1)–C(7)–N(2)	113.0(7)
Cl(1)–Fe–N(5)	87.5(2)	Cl(2)–Fe–N(5)	107.9(2)	N(1)–C(7)–C(8)	121.1(7)	N(2)–C(7)–C(8)	125.9(7)
Cl(3)–Fe–N(5)	91.7(2)	N(1)–Fe–N(5)	147.9(2)	N(3)–C(8)–C(7)	106.6(6)	N(3)–C(9)–C(10)	106.9(6)
N(3)–Fe–N(5)	74.6(2)	Fe–N(1)–C(1)	136.2(5)	N(4)–C(10)–N(5)	112.6(6)	N(4)–C(10)–C(9)	125.4(6)
Fe–N(1)–C(7)	117.8(5)	C(1)–N(1)–C(7)	105.6(6)	N(5)–C(10)–C(9)	121.9(7)	N(4)–C(11)–C(12)	132.3(7)
C(6)–N(2)–C(7)	107.1(6)	Fe–N(3)–C(8)	106.0(4)	N(4)–C(11)–C(16)	106.5(6)	C(12)–C(11)–C(16)	121.0(7)
Fe–N(3)–C(9)	107.0(4)	C(8)–N(3)–C(9)	114.1(6)	C(11)–C(12)–C(13)	116.7(8)	C(12)–C(13)–C(14)	122.1(8)
Fe–N(3)–C(17)	111.0(4)	C(8)–N(3)–C(17)	110.7(6)	C(13)–C(14)–C(15)	121.1(7)	C(14)–C(15)–C(16)	117.1(7)
C(9)–N(3)–C(17)	108.1(6)	C(10)–N(4)–C(11)	107.0(6)	N(5)–C(16)–C(11)	107.1(6)	N(5)–C(16)–C(15)	131.0(7)
Fe–N(5)–C(10)	118.2(5)	Fe–N(5)–C(16)	134.5(5)	C(11)–C(16)–C(15)	121.9(7)		
C(10)–N(5)–C(16)	106.8(6)	N(1)–C(1)–C(2)	130.6(7)				

Table 6. Final fractional atomic co-ordinates ($\times 10^4$) for complex (**2**), with estimated standard deviations in parentheses

Atom	*x*	*y*	*z*
Fe	1 990(1)	1 433(1)	2 154(1)
Cl(1)	2 620(2)	2 920(1)	2 653(1)
Cl(2)	3 131(2)	980(1)	3 630(1)
Cl(3)	1 443(2)	6(1)	1 684(1)
O(1)	−3 474(7)	3 864(4)	1 585(6)
N(1)	40(6)	1 689(4)	2 401(4)
N(2)	−1 827(6)	2 511(4)	2 203(5)
N(3)	831(6)	2 142(4)	766(4)
N(4)	4 003(6)	1 906(4)	−156(4)
N(5)	3 402(6)	1 519(4)	1 219(4)
C(1)	−774(7)	1 412(5)	3 066(5)
C(2)	−608(9)	722(6)	3 714(6)
C(3)	−1 644(10)	590(7)	4 260(6)
C(4)	−2 790(10)	1 129(7)	4 138(7)
C(5)	−2 973(9)	1 803(7)	3 503(7)
C(6)	−1 942(8)	1 937(5)	2 952(6)
C(7)	−649(7)	2 319(5)	1 900(5)
C(8)	−112(8)	2 763(5)	1 102(5)
C(9)	1 880(7)	2 566(5)	288(5)
C(10)	3 084(7)	1 985(5)	443(5)
C(11)	5 009(7)	1 353(4)	284(5)
C(12)	6 165(8)	1 009(5)	−11(6)
C(13)	6 921(8)	430(5)	600(6)
C(14)	6 568(8)	196(5)	1 496(6)
C(15)	5 412(7)	521(5)	1 777(5)
C(16)	4 629(7)	1 091(5)	1 154(5)
C(17)	84(8)	1 502(5)	89(6)
C(18)	−4 834(10)	3 842(7)	1 269(8)

Atoms O(1) and C(18) comprise the methanol molecule of solvation.

$(\mu\text{-}C_6H_5CO_2)_2]^{2+}$ species (**11**).[24] It was hoped that the bulk of bridging pivalate groups would induce a distortion in the molecule that would affect the magnetic and spectroscopic properties of the complex. Unfortunately the bond lengths and angles of (**3**) differ only slightly from those of (**11**).

The two iron(III) ions are equivalent due to a crystallographic C_2 axis through the oxo group and the midpoint of the Fe · · · Fe′ vector. As expected the longest Fe–N distance is to the central nitrogen of the ligand, *trans* to the oxo group:

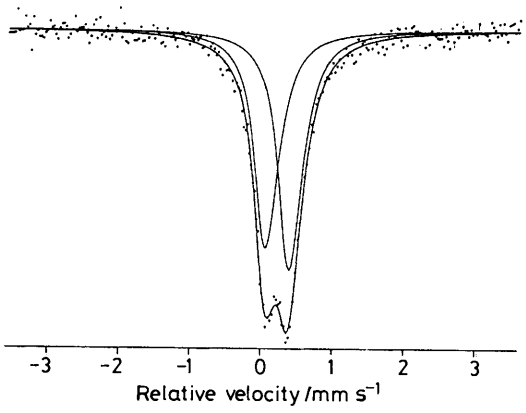

Figure 5. Room-temperature ^{57}Fe Mössbauer spectrum of complex (**2**)

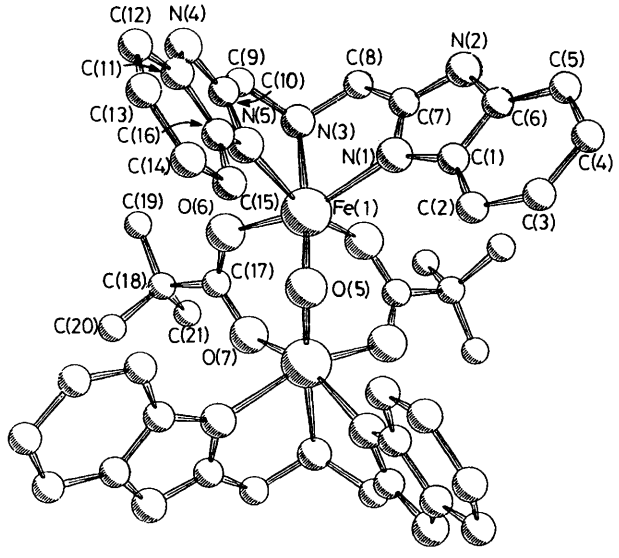

Figure 6. Molecular structure of complex (**3**). Selected bond lengths and angles are given in Table 7

Table 7. Selected bond lengths (Å) and angles (°) for complex (**3**) with standard deviations in parentheses

Fe(1)–O(5)	1.803(6)	Fe(1)–O(6)	2.046(10)	C(1)–C(2)	1.412(19)	C(1)–C(6)	1.386(18)
Fe(1)–N(1)	2.143(10)	Fe(1)–N(3)	2.300(10)	C(2)–C(3)	1.365(24)	C(3)–C(4)	1.406(27)
Fe(1)–N(5)	2.109(10)	Fe(1)–O(7)*	2.050(9)	C(4)–C(5)	1.367(26)	C(5)–C(6)	1.365(20)
O(6)–C(17)	1.277(15)	O(7)–C(17)	1.290(14)	C(7)–C(8)	1.497(19)	C(9)–C(10)	1.516(17)
N(1)–C(1)	1.395(15)	N(1)–C(7)	1.332(16)	C(11)–C(12)	1.426(20)	C(11)–C(16)	1.397(19)
N(2)–C(6)	1.425(17)	N(2)–C(7)	1.359(17)	C(12)–C(13)	1.352(22)	C(13)–C(14)	1.390(23)
N(3)–C(8)	1.460(19)	N(3)–C(9)	1.474(17)	C(14)–C(15)	1.391(20)	C(15)–C(16)	1.390(18)
N(4)–C(10)	1.356(16)	N(4)–C(11)	1.365(18)	C(17)–C(18)	1.494(21)	C(18)–C(19)	1.484(25)
N(5)–C(10)	1.316(15)	N(5)–C(16)	1.404(16)	C(18)–C(20)	1.463(33)	C(18)–C(21)	1.511(30)
O(5)–Fe(1)–O(6)	97.6(3)	O(5)–Fe(1)–N(1)	107.0(3)	C(3)–C(4)–C(5)	120.1(17)	C(4)–C(5)–C(6)	116.6(15)
O(6)–Fe(1)–N(1)	155.3(4)	O(5)–Fe(1)–N(3)	175.5(3)	N(2)–C(6)–C(1)	103.2(11)	N(2)–C(6)–C(5)	132.1(13)
O(6)–Fe(1)–N(3)	78.8(4)	N(1)–Fe(1)–N(3)	76.7(4)	C(1)–C(6)–C(5)	124.7(13)	N(1)–C(7)–N(2)	112.5(11)
O(5)–Fe(1)–N(5)	101.5(4)	O(6)–Fe(1)–N(5)	89.7(4)	N(1)–C(7)–C(8)	122.5(12)	N(2)–C(7)–C(8)	125.0(12)
N(1)–Fe(1)–N(5)	87.7(4)	N(3)–Fe(1)–N(5)	75.8(4)	N(3)–C(8)–C(7)	111.1(11)	N(3)–C(9)–C(10)	107.8(10)
O(5)–Fe(1)–O(7)*	100.5(3)	O(6)–Fe(1)–O(7)*	89.9(4)	N(4)–C(10)–N(5)	113.2(10)	N(4)–C(10)–C(9)	124.7(11)
N(1)–Fe(1)–O(7)*	83.4(4)	N(3)–Fe(1)–O(7)*	82.4(3)	N(5)–C(10)–C(9)	122.0(11)	N(4)–C(11)–C(12)	134.7(14)
N(5)–Fe(1)–O(7)*	157.8(4)	Fe(1)–O(5)–Fe(1)*	117.0(6)	N(4)–C(11)–C(16)	107.1(12)	C(12)–C(11)–C(16)	118.1(13)
Fe(1)–O(6)–C(17)	126.1(8)	C(17)–O(7)–Fe(1)*	129.4(7)	C(11)–C(12)–C(13)	120.0(15)	C(12)–C(13)–C(14)	120.2(14)
Fe(1)–N(1)–C(1)	139.5(8)	Fe(1)–N(1)–C(7)	115.8(8)	C(13)–C(14)–C(15)	122.5(14)	C(14)–C(15)–C(16)	116.5(13)
C(1)–N(1)–C(7)	104.5(10)	C(6)–N(2)–C(7)	107.8(10)	N(5)–C(16)–C(11)	107.9(11)	N(5)–C(16)–C(15)	129.5(12)
Fe(1)–N(3)–C(8)	111.4(8)	Fe(1)–N(3)–C(9)	110.2(7)	C(11)–C(16)–C(15)	122.6(12)	O(6)–C(17)–O(7)	122.5(10)
C(8)–N(3)–C(9)	113.9(10)	C(10)–N(4)–C(11)	106.5(11)	O(6)–C(17)–C(18)	118.2(11)	O(7)–C(17)–C(18)	119.2(11)
Fe(1)–N(5)–C(10)	116.9(8)	Fe(1)–N(5)–C(16)	137.9(8)	C(17)–C(18)–C(19)	114.4(14)	C(17)–C(18)–C(20)	107.9(17)
C(10)–N(5)–C(16)	105.3(10)	N(1)–C(1)–C(2)	129.1(12)	C(19)–C(18)–C(20)	110.6(17)	C(17)–C(18)–C(21)	108.6(16)
N(1)–C(1)–C(6)	112.1(11)	C(2)–C(1)–C(6)	118.7(12)	C(19)–C(18)–C(21)	106.1(18)	C(20)–C(18)–C(21)	109.1(20)
C(1)–C(2)–C(3)	116.3(14)	C(2)–C(3)–C(4)	123.5(16)				

* Atom generated by the symmetry operation $0.5 - x, -0.5 - y, z$.

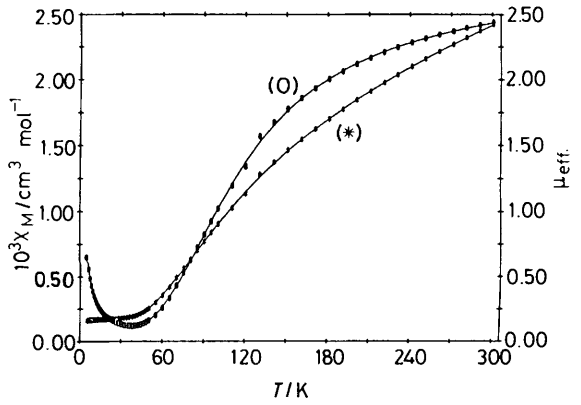

Figure 7. Molar susceptibility (○) and effective magnetic moment (*) of (**3**) as a function of temperature. The solid lines are the theoretical values as indicated in the text

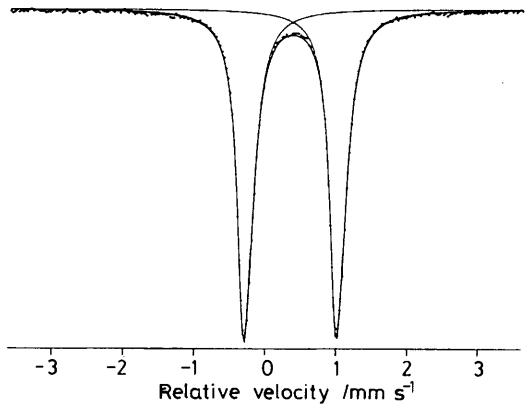

Figure 8. Mössbauer spectrum of complex (**3**) at 70 K

Fe–N(benzimidazole) 2.109, 2.143; Fe–N(amine) 2.300 Å. In the triply bridged core the bond lengths and angles are comparable to those of other models for azidomethaemerythrin: Fe–O(oxo) 1.803; Fe–O(pivalate) 2.046, 2.050; Fe···Fe′ 3.075 Å; and Fe–O(oxo)–Fe′ 117.0°.

In the i.r. spectrum (KBr disc) the symmetric and antisymmetric stretching modes of the pivalate groups occur at 1 425 and 1 550 cm^{-1} respectively. By comparison with similar model compounds, the Fe–O(oxo)–Fe′ asymmetric stretching mode is tentatively assigned at 745 cm^{-1} whereas the symmetric mode is readily assignable at 550 cm^{-1}. The electronic spectrum (CH_3CN) comprises four major bands: $\lambda_{max.}$ = 600 (ε = 87), 522 (103), 488 (257), and 356 nm (4 054 dm^3 mol^{-1} cm^{-1} per Fe). These are comparable with the spectra of other similar dinuclear iron(III) complexes and with metazidohaemerythrin itself.[10] The positive-ion f.a.b. mass spectrum shows a parent peak at *m/z* 983 corresponding to $[Fe_2L^1{}_2(\mu\text{-}O)\{\mu\text{-}(CH_3)_3CCO_2\}_2(ClO_4)]^+$.

Magnetic susceptibility data for complex (**3**) were collected in the range 5—300 K and were corrected for a small amount of mononuclear iron(III) $S = \frac{5}{2}$ paramagnetic impurities (0.07%). The data fit a dinuclear, antiferromagnetically coupled, high-spin, iron(III) system with g = 2.04, t.i.p. = 24 × 10^{-6} cm^3 mol^{-1}, and J = −116 cm^{-1}. Plots of molar magnetic susceptibility (χ_M) and effective magnetic moment ($\mu_{eff.}$) as a function of temperature are shown in Figure 7. The solid lines represent the calculated fits.

Of the seven complexes containing the $[Fe_2(\mu\text{-}O)(\mu\text{-}RCO_2)_2]^{2+}$ core for which magnetic studies have been carried out, the J values all occur in the narrow range 115—132 cm^{-1}. It is apparent from the data that there is a correlation between the Fe···Fe′ distance and the magnitude of the coupling; the greater the inter-iron distance the stronger is the coupling. This relationship is mediated by the Fe–O(oxo)–Fe′ angle; greater coupling being a result of a more linear arrangement,[25] the consequence of which is a longer Fe···Fe′ distance (Table 9). Magnetic studies of azidomethaemerythrin have not yet been

reported, but for methaemerythrin in which the Fe···Fe′ distance is 3.21 Å, $J = -134$ cm^{-1}. The inter-iron distance in azidomethaemerythrin is slightly longer at 3.25 Å, indicating that stronger coupling can be expected for this form of the metalloprotein. All the model compounds thus far reported have the drawback of relatively short Fe···Fe′ distances. The use of ligand systems which favour significantly longer inter-iron distances is now necessary to add usefully to the understanding of metalloproteins containing the $[Fe_2(\mu\text{-O})(\mu\text{-RCO}_2)_2]^{2+}$ moiety.

The room-temperature Mössbauer spectrum of complex (**3**) consists of a slightly asymmetric quadrupole doublet [fitted in a similar manner to (**10**)] with isomer shift, $\delta = 0.44(1)$ mm s^{-1}, and quadrupole splitting, $\Delta E_Q = 1.37(2)$ mm s^{-1}. As the absorber temperature is lowered the components of the quadrupole pair become more equal in intensity. At 70 K the spectrum can be fitted to a symmetrical doublet with isomer shift, $\delta = 0.55(1)$ mm s^{-1}, and quadrupole splitting, $\Delta E_Q = 1.30(2)$ mm s^{-1} (Figure 8). The difference in isomer shifts may be accounted for by the second-order Doppler shift (s.o.d.s.) arising from the different source and absorber temperatures. These values are similar to those observed for azidomethaemerythrin and other dinuclear iron(III) model compounds (Table 10). The isomer shift is typical of high-spin iron(III) and the greater quadrupole splitting compared to the mononuclear complex $[FeL^1Cl_3]$ is due to the O^{2-} ligand producing a large electric field gradient at the iron nucleus. This quadrupole splitting, however, is less than observed for the other model complexes indicating a more symmetrical charge distribution around the iron nuclei in (**3**), the reason for which is not clear.

The bridging carboxylates in (**3**) are labile in solution and are readily exchanged. Thus reaction of an acetonitrile solution of (**3**) with excess of benzoic or acetic acid, followed by reisolation of the dinuclear complex after *ca.* 5 min, gives the benzoate or acetate homologues of (**3**) in near-quantitative yields.

Table 8. Final fractional atomic co-ordinates ($\times 10^4$) for complex (**3**), with estimated standard deviations in parentheses

Atom	*x*	*y*	*z*
Fe(1)	−1 470(1)	2 647(1)	1 293(1)
Cl(1)	2 593(3)	4 808(3)	1 658(2)
O(1)	2 102(9)	5 549(10)	1 406(7)
O(2)	3 497(7)	5 067(9)	1 765(5)
O(3)	2 538(7)	4 059(8)	1 287(4)
O(4)	2 127(11)	4 618(14)	2 100(5)
O(5)	−2 500	2 500	911(4)
O(6)	−1 569(6)	1 504(6)	1 757(4)
O(7)	−3 063(5)	1 592(6)	1 930(3)
N(1)	−884(6)	3 905(7)	1 039(4)
N(2)	162(7)	4 988(8)	1 141(4)
N(3)	−140(6)	2 714(7)	1 776(4)
N(4)	840(7)	1 365(8)	662(4)
N(5)	−519(6)	1 989(7)	791(4)
C(1)	−1 062(8)	4 616(8)	681(5)
C(2)	−1 748(10)	4 691(11)	286(5)
C(3)	−1 743(12)	5 461(13)	−20(7)
C(4)	−1 102(14)	6 157(14)	43(7)
C(5)	−432(13)	6 077(10)	422(7)
C(6)	−425(9)	5 301(9)	722(5)
C(7)	−146(9)	4 166(9)	1 307(5)
C(8)	258(10)	3 618(11)	1 756(5)
C(9)	479(9)	1 989(10)	1 600(5)
C(10)	260(8)	1 767(9)	1 014(5)
C(11)	385(10)	1 282(10)	183(6)
C(12)	604(11)	930(11)	−339(5)
C(13)	−6(12)	982(12)	−747(6)
C(14)	−847(10)	1 379(10)	−659(6)
C(15)	−1 093(9)	1 751(9)	−163(5)
C(16)	−465(9)	1 680(8)	254(5)
C(17)	−2 280(8)	1 223(8)	1 999(4)
C(18)	−2 193(11)	436(11)	2 376(7)
C(19)	−1 246(12)	158(12)	2 488(9)
C(20)	−2 709(21)	−318(18)	2 146(13)
C(21)	−2 598(20)	695(21)	2 917(9)

Conclusion

Mononuclear and dinuclear complexes of the flexible ligands L^1 and L^2 containing the biologically relevant imidazole moiety have been prepared. Both meridional and facial co-ordination of the ligands have been observed. Although L^1 forms the stable, discrete, mononuclear complex (**1**) with manganese(II) acetate, the presence of benzoate anions results in partial aerial oxidation and the preferred formation of the mixed-valence hexanuclear complex (**9**). The dinuclear iron(III) complex (**3**) contains the $[Fe_2(\mu\text{-O})(\mu\text{-RCO}_2)_2]^{2+}$ core and is a model for azidomethaemerythrin. It has been shown that this core system can be assembled either directly from its individual components or from the $FeCl_3$ adduct (**10**). Attempts to prepare the manganese(III) analogue of (**3**) were unsuccessful.

Table 10. Mössbauer parameters for metazidohaemerythrin (δ 0.50, ΔE_Q 1.91 mm s^{-1} at 77 K) and dinuclear iron(III) model complexes containing the $[Fe_2(\mu\text{-O})(\mu\text{-RCO}_2)_2]^{2+}$ core

	T/K	δ[a]/mm s^{-1}	ΔE_Q/mm s^{-1}
(**3**)[b]	293	0.44(1)	1.37(2)
	70	0.55(1)	1.30(2)
(**4**)[c]	80	0.46(3)	1.72(5)
(**5**)[c]	77	0.47(3)	1.50(5)
	4.2	0.47(3)	1.50(5)
(**6**)[d]	4.2	0.52(3)	1.60
(**7**)[e]	77[f]	0.48	1.27
	4.2[g]	0.48	1.39

[a] Relative to metallic iron at room temperature. [b] This work. [c] Ref. 9. [d] Ref. 10. [e] Ref. 11. [f] Values for the ClO_4^- salt of the 1,3-diaminobutane ligand L^6. [g] Values for the ClO_4^- salt of the 1,3-diaminopropane ligand L^7.

Table 9. Correlation of structural and magnetic features of model complexes containing the $[Fe_2(\mu\text{-O})(\mu\text{-RCO}_2)_2]^{2+}$ core

Complex	Fe···Fe′/Å	Fe–O(oxo)/Å	Fe–O(oxo)–Fe′/°	J/cm^{-1}
(**4**)[a]	3.063(5)	1.77(2), 1.80(2)	118.3(5)	−115[b]
(**3**)[c]	3.075(5)	1.803(6)	117.0(6)	−116
(**11**)[d]	3.079(2)	1.777(5), 1.802(6)	118.7(3)	−117(1)
(**5**)[b]	3.12(4)	1.800(3)	119.7(1)	−119(1)
(**7**)[a]	3.129(2)	1.794(3)	121.3(3)	−120[f]
(**6**)[g]	3.145 7(6)	1.780(2), 1.788(2)	123.6(1)	−121(1)
(**8**)[h]	3.151(1)	1.783(4), 1.787(4)	123.9(2)	−132

[a] Ref. 8. [b] Ref. 9. [c] This work. [d] Ref. 24. [e] Ref. 11. [f] Value for the ClO_4^- salt of the 1,3-diaminopropane ligand L^7. [g] Ref. 10. [h] Ref. 12.

Acknowledgements

We acknowledge the S.E.R.C. for the award of a studentship (to J. D. C.) and the S.E.R.C. and the Royal Society for asssistance in the purchase of the diffractometer and computing facilities.

References

1 S. J. Lippard, *Angew. Chem., Int. Ed. Engl.*, 1988, **27**, 344 and refs. therein.
2 J. E. Sheats, R. S. Czernuszewicz, G. C. Dismukes, A. L. Rheingold, V. Petrouleas, J-A. Stubbe, W. H. Armstrong, R. H. Beer, and S. J. Lippard, *J. Am. Chem. Soc.*, 1987, **109**, 1435 and refs. therein.
3 A. W. Rutherford, *Trends Biochem. Sci.*, 1989, **14**, 227.
4 B. Chiswell, E. D. McKenzie, and L. F. Lindoy, in 'Comprehensive Co-ordination Chemistry,' vol. 4, eds. G. Wilkinson, R. D. Gillard, and J. A. McCleverty, Pergamon, Oxford, 1987, p. 26.
5 M. E. Fernandopulle, P. A. Gillespie, and W. R. McWhinnie, *Inorg. Chim. Acta*, 1978, **29**, 197.
6 W. M. Reiff, W. A. Baker, jun., and N. E. Erickson, *J. Am. Chem. Soc.*, 1968, **90**, 4794.
7 R. E. Stenkamp, L. C. Sieker, and L. H. Jensen, *J. Am. Chem. Soc.*, 1984, **106**, 618.
8 K. Wieghardt, K. Pohl, and W. Gebert, *Angew. Chem., Int. Ed. Engl.*, 1983, **22**, 727.
9 J-A. Hartman, R. L. Rardin, P. Chaudhuri, K. Pohl, K. Wieghardt, B. Nuber, J. Weiss, G. C. Papaefthymiou, R. B. Frankel, and S. J. Lippard, *J. Am. Chem. Soc.*, 1987, **109**, 7387.
10 W. H. Armstrong, A. Spool, G. C. Papaefthymiou, R. B. Frankel, and S. J. Lippard, *J. Am. Chem. Soc.*, 1984, **106**, 3653.
11 H. Toftlund, K. S. Murray, P. R. Zwack, L. F. Taylor, and O. P. Anderson, *J. Chem. Soc., Chem. Commun.*, 1986, 191.
12 J. B. Vincent, J. C. Huffman, G. Christou, Q. Li, M. A. Nanny, D. N. Hendrickson, R. H. Fong, and R. H. Fish, *J. Am. Chem. Soc.*, 1988, **110**, 6898.
13 'Vogel's Textbook of Practical Organic Chemistry,' 4th edn., Longman, London, 1978, p. 661.
14 A. F. Childs, L. J. Goldsworthy, G. F. Harding, F. E. King, A. W. Nineham, W. L. Norris, S. G. P. Plant, B. Selton, and A. L. L. Tompsett, *J. Chem. Soc.*, 1948, 2174.
15 C. J. O'Connor, *Prog. Inorg. Chem.*, 1982, **29**, 203.
16 G. M. Sheldrick, SHELXTL System for Crystal Structure Solution, University of Göttingen, 1983, revision 4.
17 K. Wieghardt, U. Bossek, J. Bonvoisoin, P. Beauvillin, J-J. Girerd, B. Nuber, J. Weiss, and J. Heinze, *Angew. Chem., Int. Ed. Engl.*, 1986, **25**, 1030.
18 A. R. E. Baikie, A. J. Howes, M. B. Hursthouse, A. B. Quick, and P. Thornton, *J. Chem. Soc., Chem. Commun.*, 1986, 1587.
19 A. R. Schake, J. B. Vincent, Q. Li, P. D. W. Boyd, K. Folting, J. C. Huffman, D. N. Hendrickson, and G. Christou, *Inorg. Chem.*, 1989, **28**, 1915.
20 J. B. Bush, jun. and H. Finkbeiner, *J. Am. Chem. Soc.*, 1968, **90**, 5903.
21 Y. Nishida, M. Takeuchi, H. Shimo, and S. Kida, *Inorg. Chim. Acta*, 1985, **96**, 115.
22 P. C. Healy, J. M. Patrick, B. W. Skelton, and A. H. White, *Aust. J. Chem.*, 1983, **36**, 2031.
23 W. M. Reiff, E. H. Witten, K. Mottle, T. F. Brennan, and A. R. Garafalo, *Inorg. Chim. Acta*, 1983, **77**, L27.
24 P. Gomez-Romero, N. Casan-Pastor, A. Ben-Hussein, and G. B. Jameson, *J. Am. Chem. Soc.*, 1988, **110**, 1988.
25 R. N. Mukerjee, D. T. P. Stack, and R. H. Holm, *J. Am. Chem. Soc.*, 1988, **110**, 1850.

Received 20*th October* 1989; *Paper* 9/04529E